

$B \rightarrow K\eta^{(\prime)}$ decays and NLO contributions in the pQCD approach

Zhen-Jun Xiao*, Zhi-Qing Zhang, Xin Liu and Libo Guo

*Department of Physics and Institute of Theoretical Physics, Nanjing Normal University,
Nanjing, Jiangsu 210097, P.R.China*

E-mail: xiaozhenjun@njnu.edu.cn

We report our calculations of the partial NLO QCD corrections to the $B \rightarrow K\eta^{(\prime)}$ decays in the perturbative QCD (pQCD) factorization approach. The NLO contributions can provide a 70% enhancement (a 30% reduction) to the leading order pQCD predictions for the branching ratios of $B \rightarrow K\eta'$ ($B \rightarrow K\eta$) decays. Such NLO contributions play the key role in understanding the observed pattern of branching ratios. The pQCD predictions for the CP asymmetries of $B \rightarrow K\eta^{(\prime)}$ decays are also consistent with currently available data.

*Flavor Physics and CP Violation 2009,
May 27 - June 1, 2009,
Lake Placid, NY, USA*

*Speaker.

1. Introduction

The unexpectedly large branching ratios for $B \rightarrow K\eta'$ decays were firstly reported in 1997 by CLEO Collaboration [1]. 12 years later, three of the four $B \rightarrow K\eta^{(\prime)}$ decays have been measured with high precision [2]. Besides the branching ratios, the CP violating asymmetries for $B^\pm \rightarrow K^\pm\eta^{(\prime)}$ and $B^0 \rightarrow K^0\eta^{(\prime)}$ decays have been measured very recently [2, 3].

In the SM the decay $B \rightarrow K\eta^{(\prime)}$ is believed to proceed dominantly through gluonic penguin processes[4] and has been evaluated by employing various methods [5, 6, 7, 8, 9, 10, 11, 12, 13, 14, 15]. Although great progress have been made during the past decade, but the predictions for $Br(B \rightarrow K\eta')$ from both the QCD factorization (QCDF) approach [13, 16] and the perturbative QCD (pQCD) approach [15, 17] are still smaller than the data.

Furthermore, there is a large disparity between the measured branching ratios: $Br(B \rightarrow K\eta') \gg Br(B \rightarrow K\eta)$. Many efforts have been made to interpret this pattern, which include, for example,

- (a) Conventional $b \rightarrow sq\bar{q}$ with constructive (destructive) interference between the $u\bar{u}$, $d\bar{d}$ and $s\bar{s}$ components of η' (η) [4];
- (b) Large intrinsic charm content of η' through the chain $b \rightarrow sc\bar{c} \rightarrow s\eta'$ [6] or through $b \rightarrow sc\bar{c} \rightarrow sg^*g^* \rightarrow s(\eta, \eta')$ due to the QCD anomaly [7];
- (c) The spectator hard-scattering mechanism through the anomalous coupling of $gg \rightarrow \eta'$ [8, 9, 10];
- (d) A significant flavor-singlet contribution [9, 13];
- (e) A strong penguin $b \rightarrow sg$ enhanced by new physics [11, 12].

In Ref. [15], the authors calculated the branching ratios of $B \rightarrow K\eta^{(\prime)}$ decays by employing the pQCD approach at leading order. They considered the large corrections from $SU(3)$ flavor symmetry breaking as well as the possible gluonic component of η' meson, but their prediction for $Br(B^0 \rightarrow K^0\eta')$ ($Br(B^0 \rightarrow K^0\eta)$) is much smaller (larger) than the measured value. A sizable gluonic content in η' meson may provide a large enhancement to the decay rate of $B \rightarrow K\eta'$. But the calculation in Ref. [18] showed that such contribution is numerically very small and can be neglected safely.

Besides the possible mechanisms mentioned above, we here consider a new and natural solution: the effects of the next-to-leading order (NLO) contributions in the pQCD approach. The NLO contributions considered here include: QCD vertex corrections, the quark-loops and the chromo-magnetic penguins. We expect that they are the major part of the full NLO contributions in pQCD approach [19].

In the pQCD approach, the decay amplitude is separated into soft (Φ_{M_i}), hard ($H(k_i, t)$), and harder ($C(M_W)$) dynamics characterized by different energy scales ($\Lambda_{QCD}, t, m_b, M_W$) [17]. The decay amplitude $\mathcal{A}(B \rightarrow M_2M_3)$ can be written conceptually as the convolution,

$$\mathcal{A}(B \rightarrow M_2M_3) \sim \int d^4k_1 d^4k_2 d^4k_3 \text{Tr}[C(t)\Phi_B(k_1)\Phi_{M_2}(k_2)\Phi_{M_3}(k_3)H(k_1, k_2, k_3, t)], \quad (1.1)$$

where k_i 's are momenta of light quarks included in each meson, and Tr denotes the trace over Dirac and color indices. $C(t)$ is the Wilson coefficient evaluated at scale t . The hard kernel $H(k_1, k_2, k_3, t)$

describes the hard dynamics, and therefore can be perturbatively calculated. The function Φ_{M_i} is the wave function.

Since the b quark inside the B meson is rather heavy, we consider the B meson at rest for simplicity. It is then convenient to use light-cone coordinate (p^+, p^-, \mathbf{p}_T) to describe the meson's momenta: $p^\pm = (p^0 \pm p^3)/\sqrt{2}$ and $\mathbf{p}_T = (p^1, p^2)$.

For the studied $B \rightarrow K\eta^{(\prime)}$ decays, the weak effective Hamiltonian H_{eff} for $b \rightarrow s$ transition can be written as [20]

$$\mathcal{H}_{eff} = \frac{G_F}{\sqrt{2}} \sum_{q=u,c} V_{qb}V_{qs}^* \left\{ [C_1(\mu)O_1^q(\mu) + C_2(\mu)O_2^q(\mu)] + \sum_{i=3}^{10} C_i(\mu) O_i(\mu) \right\}. \quad (1.2)$$

where $G_F = 1.16639 \times 10^{-5} GeV^{-2}$ is the Fermi constant, and V_{ij} is the CKM matrix element, $C_i(\mu)$ are the Wilson coefficients evaluated at the renormalization scale μ and $O_i(\mu)$ are the four-fermion operators.

In PQCD approach, the energy scale “ t ” is chosen as the largest energy scale in the hard kernel $H(x_i, b_i, t)$ of a given Feynman diagram, in order to suppress the higher order corrections and improve the reliability of the perturbative calculation. Here, the scale “ t ” may be larger or smaller than the m_b scale. In the range of $t < m_b$ or $t \geq m_b$, the number of active quarks is $N_f = 4$ or $N_f = 5$, respectively. The explicit expressions of the LO and NLO $C_i(m_W)$ can be found easily, for example, in Refs. [21, 20]. For the expressions of the wave functions of B meson and the relevant distribution functions of the K and (η, η') mesons, one can see Ref. [21, 22]. The Gegenbauer moments are the following [23]:

$$a_1^K = 0.2, \quad a_2^K = 0.25, \quad a_4^K = -0.015. \quad (1.3)$$

The values of other parameters are $\eta_3 = 0.015$ and $\omega = -3.0$.

For the mixing of the $\eta - \eta'$ system, we use the quark-flavor mixing scheme, where the physical states η and η' are related to the flavor states $\eta_q = (u\bar{u} + d\bar{d})/\sqrt{2}$ and $\eta_s = s\bar{s}$ through a single mixing angle ϕ ,

$$\begin{pmatrix} \eta \\ \eta' \end{pmatrix} = \begin{pmatrix} \cos \phi & -\sin \phi \\ \sin \phi & \cos \phi \end{pmatrix} \begin{pmatrix} \eta_q \\ \eta_s \end{pmatrix} = \begin{pmatrix} F_1(\phi)(u\bar{u} + d\bar{d}) + F_2(\phi) s\bar{s} \\ F'_1(\phi)(u\bar{u} + d\bar{d}) + F'_2(\phi) s\bar{s} \end{pmatrix} \quad (1.4)$$

with $F_1(\phi) = \cos \phi/\sqrt{2}$, $F_2(\phi) = -\sin \phi$, $F'_1(\phi) = \sin \phi/\sqrt{2}$ and $F'_2(\phi) = \cos \phi$. The distribution amplitudes $\phi_{\eta_q}^{A,P,T}$ represent the axial vector, pseudoscalar and tensor component of the wave function respectively [23], and can be found in Ref.[22].

2. Decay amplitudes at leading order

At the leading order in pQCD approach, the Feynman diagrams as shown in Fig. 1 may contribute to $B \rightarrow K\eta^{(\prime)}$ decays. From the factorizable emission diagrams 1(a) and 1(b), the corresponding form factors can be extracted by perturbative calculation. For Fig.1(a) and 1(b) with the $B \rightarrow K$ transition, the operators $O_{1,2}$, $O_{3,4}$ and $O_{9,10}$ are $(V - A)(V - A)$ currents, the sum of the

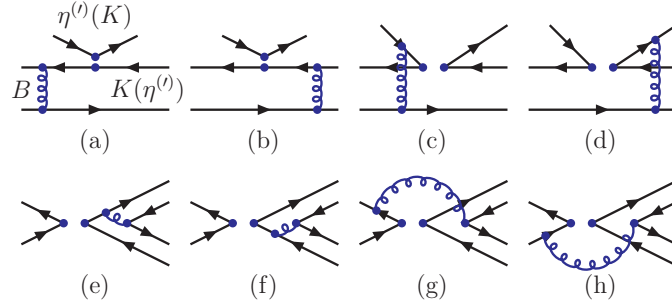


Figure 1: Feynman diagrams which may contribute to the $B \rightarrow K\eta^{(\prime)}$ decays at leading order.

individual amplitudes is given as

$$F_{eK} = \frac{8}{\sqrt{2}} \pi G_F C_F m_B^4 \int_0^1 dx_1 dx_2 \int_0^\infty b_1 db_1 b_2 db_2 \phi_B(x_1, b_1) \times \left\{ [(1+x_2)\phi_K^A(\bar{x}_2) + (1-2x_2)r_K(\phi_K^P(\bar{x}_2) - \phi_K^T(\bar{x}_2))] \cdot E_e(t_a)h_e(x_1, x_2, b_1, b_2) + 2r_K\phi_K^P(\bar{x}_2) \cdot E_e(t'_a)h_e(x_2, x_1, b_2, b_1) \right\}, \quad (2.1)$$

where $r_K = m_0^K/m_B$ with m_0^K is the chiral scale; $C_F = 4/3$ is a color factor, and $\bar{x}_2 = 1 - x_2$. The evolution function $E_e(t)$ and hard function h_e can be found in Ref. [22]. Also from diagrams 1(a) and 1(b), the decay amplitudes corresponding to the $(V-A)(V+A)$ and/or $(S-P)(S+P)$ currents are the following

$$F_{eK}^{P1} = -F_{eK}, \quad (2.2)$$

$$F_{eK}^{P2} = \frac{16}{\sqrt{2}} \pi G_F C_F m_B^4 \int_0^1 dx_1 dx_2 \int_0^\infty b_1 db_1 b_2 db_2 \phi_B(x_1) \times \left\{ r_\eta [\phi_K^A(\bar{x}_2) + r_K((2+x_2)\phi_K^P(\bar{x}_2) + x_2\phi_K^T(\bar{x}_2))] \cdot E_e(t_a)h_e(x_1, x_2, b_1, b_2) + 2r_K r_\eta \phi_K^P(\bar{x}_2) \cdot E_e(t'_a)h_e(x_2, x_1, b_2, b_1) \right\}. \quad (2.3)$$

From Fig. 1, one can find the corresponding decay amplitudes: $(M_{eK}, M_{eK}^{P1, P2})$ (1(c) and 1(d)), $(M_{aK}, M_{aK}^{P1, P2})$ (1(e) and 1(f)) and $(F_{aK}, F_{aK}^{P1, P2})$ (1(g) and 1(h)) [22]. By exchanging position of the K and $\eta^{(\prime)}$ in Fig. 1, one can find the corresponding decay amplitudes for the new diagrams easily[22]: $(F_{e\eta}, F_{e\eta}^{P1, P2})$, $(M_{e\eta}, M_{e\eta}^{P1, P2})$, $(M_{a\eta}, M_{a\eta}^{P1, P2})$, and $(F_{a\eta}, F_{a\eta}^{P1, P2})$.

For the two $B \rightarrow K\eta$ decays, the total decay amplitude with the inclusion of the corresponding Wilson coefficients can be finally written as

$$\begin{aligned} \mathcal{M}(K^0\eta) = \langle K^0\eta | H_{eff} | B^0 \rangle = & F_{eK} \left\{ \left[\xi_u a_2 - \xi_t \left(2a_3 - 2a_5 - \frac{1}{2}a_7 + \frac{1}{2}a_9 \right) \right] f_\eta^q \right. \\ & \left. - \xi_t \left(a_3 + a_4 - a_5 + \frac{1}{2}a_7 - \frac{1}{2}a_9 - \frac{1}{2}a_{10} \right) f_\eta^s \right\} - F_{e\eta} \xi_t \left(a_4 - \frac{1}{2}a_{10} \right) f_K F_1(\phi) \\ & - \left[F_{eK}^{P2} f_\eta^s + F_{e\eta}^{P2} f_K F_1(\phi) \right] \xi_t \left(a_6 - \frac{1}{2}a_8 \right) - \left[F_{aK} F_2(\phi) + F_{a\eta} F_1(\phi) \right] \xi_t \left(a_4 - \frac{1}{2}a_{10} \right) \\ & + \left[F_{aK}^{P2} F_2(\phi) + F_{a\eta}^{P2} F_1(\phi) \right] \xi_t \left(a_6 - \frac{1}{2}a_8 \right) f_B \end{aligned}$$

$$\begin{aligned}
 & +M_{eK} \left\{ \left[\xi_u C_2 - \xi_t \cdot \left(2C_4 + \frac{1}{2}C_{10} \right) \right] F_1(\phi) - \xi_t \left(C_3 + C_4 - \frac{1}{2}C_9 - \frac{1}{2}C_{10} \right) F_2(\phi) \right\} \\
 & -M_{e\eta} \xi_t \left(C_3 - \frac{1}{2}C_9 \right) F_1(\phi) - [M_{eK}^{P1} F_2(\phi) + M_{e\eta}^{P1} F_1(\phi)] \xi_t \left(C_5 - \frac{1}{2}C_7 \right) \\
 & -M_{eK}^{P2} \xi_t \left[\left(2C_6 + \frac{1}{2}C_8 \right) F_1(\phi) + \left(C_6 - \frac{1}{2}C_8 \right) F_2(\phi) \right], \tag{2.4}
 \end{aligned}$$

$$\begin{aligned}
 \mathcal{M}(K^+ \eta) = & \langle K^+ \eta | H_{eff} | B^0 \rangle = F_{eK} \left\{ \left[\xi_u a_2 - \xi_t \left(2a_3 - 2a_5 - \frac{1}{2}a_7 + \frac{1}{2}a_9 \right) \right] f_\eta^q \right. \\
 & - \xi_t \left(a_3 + a_4 - a_5 + \frac{1}{2}a_7 - \frac{1}{2}a_9 - \frac{1}{2}a_{10} \right) f_\eta^s \left. \right\} + \{ F_{e\eta} F_1(\phi) f_K + [F_{a\eta} F_1(\phi) \\
 & + F_{aK} F_2(\phi)] f_B \} \xi_u a_1 - [F_{e\eta} F_1(\phi) f_K + (F_{a\eta} F_1(\phi) + F_{aK} F_2(\phi)) f_B] \xi_t (a_4 + a_{10}) \\
 & - [F_{e\eta}^{P2} F_1(\phi) f_K + (F_{a\eta}^{P2} F_1(\phi) + F_{aK}^{P2} F_2(\phi)) f_B] \xi_t (a_6 + a_8) - F_{eK}^{P2} f_\eta^s \xi_t \left(a_6 - \frac{1}{2}a_8 \right) \\
 & - M_{eK}^{P1} \xi_t \left(C_5 - \frac{1}{2}C_7 \right) + M_{eK} \left\{ \left[\xi_u C_2 - \xi_t \left(2C_4 + \frac{1}{2}C_{10} \right) \right] F_1(\phi) \right. \\
 & - \xi_t \left(C_3 + C_4 - \frac{1}{2}C_9 - \frac{1}{2}C_{10} \right) F_2(\phi) \left. \right\} - [M_{aK}^{P1} F_2(\phi) + (M_{e\eta}^{P1} + M_{a\eta}^{P1}) F_1(\phi)] \\
 & \times \xi_t (C_5 + C_7) + [M_{aK} F_2(\phi) + (M_{e\eta} + M_{a\eta}) F_1(\phi)] [\xi_u C_1 - \xi_t (C_3 + C_9)] \\
 & - M_{eK}^{P2} \xi_t \left[\left(2C_6 + \frac{1}{2}C_8 \right) F_1(\phi) + \left(C_6 - \frac{1}{2}C_8 \right) F_2(\phi) \right]. \tag{2.5}
 \end{aligned}$$

where $\xi_u = V_{ub}^* V_{us}$, $\xi_t = V_{tb}^* V_{ts}$, the coefficients a_i are the combinations of the Wilson coefficients C_i , and have been defined as usual

$$a_{1,2} = C_{2,1} + \frac{C_{1,2}}{3}; \quad a_i = C_i + \frac{C_{i+1}}{3}, i = 3, 5, 7, 9; \quad a_i = C_i + \frac{C_{i-1}}{3}, i = 4, 6, 8, 10. \tag{2.6}$$

The total decay amplitudes for the two $B \rightarrow K\eta^{(\prime)}$ decays can be obtained easily from Eqs.(2.4) and (2.5) by the following replacements

$$f_\eta^d \rightarrow f_{\eta'}^d, \quad f_\eta^s \rightarrow f_{\eta'}^s, \quad F_1(\phi) \rightarrow F_1'(\phi), \quad F_2(\phi) \rightarrow F_2'(\phi). \tag{2.7}$$

3. NLO contributions in pQCD approach

At the NLO level, the following changes or contributions should be considered:

- The NLO Wilson coefficients $C_i(m_W)$, the NLO RG evolution matrix and the $\alpha_s(t)$ at two-loop level should be used.
- The NLO hard kernel $H^{(1)}(\alpha_s^2)$ should be included. All the Feynman diagrams, which may contribute to the hard kernel H at the order of α_s^2 , as illustrated by Figs. 2-5, should be considered.

At present, the calculations for the vertex corrections, the quark-loops and chromo-magnetic penguins, in relevant with $B \rightarrow K\eta^{(\prime)}$ decays as shown in Fig. 2, have been done in Ref. [22]. For

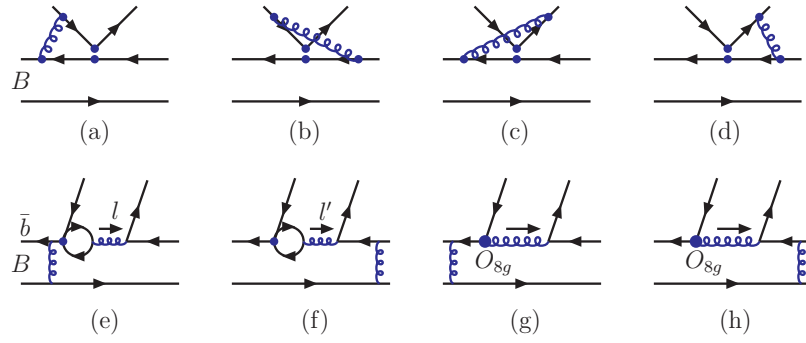


Figure 2: The Feynman diagrams in relevant with the NLO vertex QCD corrections, the quark-loops and charmo-magnetic penguins for $B \rightarrow K\eta^{(\prime)}$ decays.

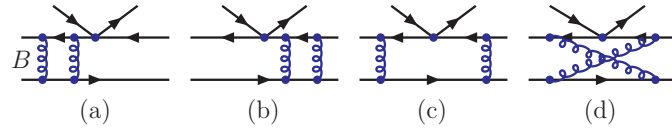


Figure 3: The typical vertex Feynman diagrams which contribute to the form factors at the NLO level.

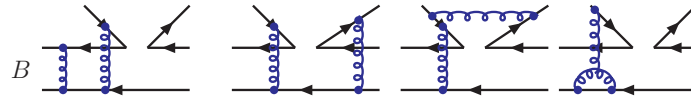


Figure 4: The typical hard spectator Feynman diagrams which contribute at the NLO level.

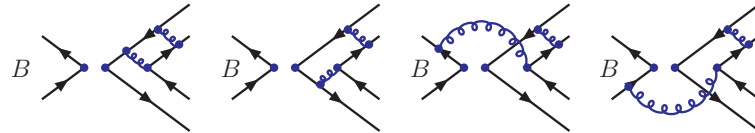


Figure 5: The typical annihilation Feynman diagrams which contribute at the NLO level.

the Feynman diagrams as shown in Figs. 3-5, however, the analytical calculations have not been completed yet.

The vertex corrections to the factorizable emission diagrams, as illustrated by Figs. 2a-2d, have been calculated years ago in the QCD factorization approach[16, 13, 14]. The difference of the calculations induced by considering or not considering the parton transverse momentum is rather small [19], say less than 10%, and therefore can be neglected. The vertex corrections can then be absorbed into the re-definition of the Wilson coefficients $a_i(\mu)$ by adding a vertex-function $V_i(M)$ to them[14, 19].

The contribution from the so-called “quark-loops” is a kind of penguin correction with the four quark operators insertion, as illustrated by Fig. 2e-2f. For the $b \rightarrow s$ transition, the contributions from the various quark loops are given by:

$$H_{eff}^{(q)} = - \sum_{q=u,c,t} \sum_{q'} \frac{G_F}{\sqrt{2}} V_{qb} V_{qs}^* \frac{\alpha_s(\mu)}{2\pi} C^q(\mu, l^2) (\bar{s} \gamma_\rho (1 - \gamma_5) T^a b) (\bar{q}' \gamma^\rho T^a q'), \quad (3.1)$$

It is straightforward to calculate the decay amplitude for Fig.2e and 2f. We found two kinds of topological decay amplitudes [22]: $M_{K\eta_s}^{(q)}$ for $B \rightarrow K$ transition and $M_{\eta_q K}^{(q)}$ for $B \rightarrow \eta$ transition. For $B \rightarrow K\eta'$ decays, we found the similar decay amplitudes. Finally, the total ‘‘quark-loop’’ contribution to the considered $B \rightarrow K\eta^{(\prime)}$ ($K = K^0, K^+$) decays can be written as [22]

$$M_{K\eta}^{(ql)} = \langle K\eta | \mathcal{H}_{eff}^{ql} | B \rangle = \frac{G_F}{\sqrt{2}} \sum_{q=u,c,t} \lambda_q \left[M_{K\eta_s}^{(q)} F_2(\phi) + M_{\eta_q K}^{(q)} F_1(\phi) \right], \quad (3.2)$$

$$M_{K\eta'}^{(ql)} = \langle K\eta' | \mathcal{H}_{eff}^{(ql)} | B \rangle = \frac{G_F}{\sqrt{2}} \sum_{q=u,c,t} \lambda_q \left[M_{K\eta_s}^{(q)} F_2'(\phi) + M_{\eta_q K}^{(q)} F_1'(\phi) \right]. \quad (3.3)$$

For the magnetic penguins, the corresponding weak effective Hamiltonian contains the $b \rightarrow sg$ transition,

$$H_{eff}^{cmp} = -\frac{G_F}{\sqrt{2}} V_{tb} V_{ts}^* C_{8g}^{eff} O_{8g}, \quad (3.4)$$

with the chromo-magnetic penguin operator,

$$O_{8g} = \frac{g_s}{8\pi^2} m_b \bar{d}_i \sigma^{\mu\nu} (1 + \gamma_5) T_{ij}^a G_{\mu\nu}^a b_j, \quad (3.5)$$

where i, j being the color indices of quarks. The corresponding effective Wilson coefficient $C_{8g}^{eff} = C_{8g} + C_5$.

The decay amplitudes, $M_{K\eta_s}^{(g)}$ and $M_{\eta_q K}^{(g)}$, have been obtained by evaluating the Feynman diagrams Figs.2g and 2h [22]. The total chromo-magnetic penguin contribution to the considered $B \rightarrow K\eta^{(\prime)}$ ($K = K^0, K^+$) decays can be written as

$$M_{K\eta}^{(cmp)} = \langle K\eta | \mathcal{H}_{eff}^{cmp} | B \rangle = -\frac{G_F}{\sqrt{2}} \lambda_t \left[M_{K\eta_s}^{(g)} F_2(\phi) + M_{\eta_q K}^{(g)} F_1(\phi) \right], \quad (3.6)$$

$$M_{K\eta'}^{(cmp)} = \langle K\eta' | \mathcal{H}_{eff}^{cmp} | B \rangle = -\frac{G_F}{\sqrt{2}} \lambda_t \left[M_{K\eta_s}^{(g)} F_2'(\phi) + M_{\eta_q K}^{(g)} F_1'(\phi) \right]. \quad (3.7)$$

4. Numerical Results and Discussions

We use the following input parameters [2, 24] in the numerical calculations

$$\begin{aligned} f_B &= 0.21\text{GeV}, & f_K &= 0.16\text{GeV}, & m_\eta &= 547.5\text{MeV}, & m_{\eta'} &= 957.8\text{MeV}, \\ m_K &= 0.49\text{GeV}, & m_{0K} &= 1.7\text{GeV}, & M_B &= 5.279\text{GeV}, & m_b &= 4.8\text{GeV}, \\ M_W &= 80.41\text{GeV}, & \tau_{B^0} &= 1.527\text{ps}, & \tau_{B^+} &= 1.643\text{ps}. \end{aligned} \quad (4.1)$$

For the CKM quark-mixing matrix elements, we use the values as given in Ref.[2, 24]:

$$\begin{aligned} V_{ud} &= 0.9745, & V_{us} &= \lambda = 0.2200, & |V_{ub}| &= 4.31 \times 10^{-3}, & V_{cd} &= -0.224, \\ V_{cd} &= 0.996, & V_{cb} &= 0.0413, & |V_{td}| &= 7.4 \times 10^{-3}, & V_{ts} &= -0.042, & V_{tb} &= 0.9991, \end{aligned} \quad (4.2)$$

with the CKM angles $\beta = 21.6^\circ$, $\gamma = 60^\circ \pm 20^\circ$ and $\alpha = 100^\circ \pm 20^\circ$.

Using the wave functions and the input parameters as specified in previous sections, it is straightforward to calculate the CP-averaged branching ratios for the considered four $B \rightarrow K\eta^{(\prime)}$

Table 1: The pQCD predictions for the branching ratios (in unit of 10^{-6}). The label LO_{NLOWC} means the LO results with the NLO Wilson coefficients, and +VC, +QL, +MP, NLO means the inclusion of the vertex corrections, the quark loops, the magnetic penguin, and all the considered NLO corrections, respectively.

Mode	LO	LO_{NLOWC}	+VC	+QL	+MP	NLO	Data	QCDF
$B^+ \rightarrow K^+ \eta$	4.7	4.7	4.3	4.9	3.1	$3.2^{+3.2}_{-1.8}$	2.6 ± 0.6	$1.9^{+3.0}_{-1.9}$
$B^+ \rightarrow K^+ \eta'$	30.2	46.8	74.6	48.1	30.2	$51.0^{+18.0}_{-10.9}$	70.5 ± 3.5	$49.1^{+45.2}_{-23.6}$
$B^0 \rightarrow K^0 \eta$	3.2	3.4	3.1	3.8	2.3	$2.1^{+2.6}_{-1.5}$	< 2.0	$1.1^{+2.4}_{-1.5}$
$B^0 \rightarrow K^0 \eta'$	31.3	46.5	69.7	48.5	20.7	$50.3^{+16.8}_{-10.6}$	68 ± 4	$46.5^{+41.9}_{-22.0}$

decays, which are listed in Table 1. For comparison, we also list the corresponding updated experimental results [2] and numerical results evaluated in the framework of the QCDF approach [14].

It is worth stressing that the theoretical predictions in the pQCD approach have relatively large theoretical errors induced by the still large uncertainties of many input parameters, such as quark masses ($m_{u,d}, m_s$), chiral scales (m_{0K}, m_0^q, m_0^s), Gegenbauer coefficients ($a_i^{(K,\eta)}, \dots$), ω_b and the CKM angles (α, γ), etc. From the numerical results about the branching ratios, one can see that

- The LO pQCD predictions for branching ratios are much smaller (larger) than the measured values for $B \rightarrow K\eta'$ ($B \rightarrow K\eta$) decays, show the same tendency as found in Ref. [15].
- The NLO contributions can interfere constructively (destructively) with the corresponding LO part for $B \rightarrow K\eta'$ ($B \rightarrow K\eta$) decays. For $B^0 \rightarrow K^0\eta'$ and $B^+ \rightarrow K^+\eta'$ decays, the NLO contributions provide a 70% enhancement to their branching ratios. For $B^0 \rightarrow K^0\eta$ and $B^+ \rightarrow K^+\eta$ decays, on the other hand, the NLO contributions give rise to a 30% reduction to their branching ratios and result in the good agreement between the pQCD predictions and the data.
- The NLO pQCD predictions for branching ratios $Br(B \rightarrow K\eta^{(\prime)})$ agree very well with the measured values within one standard deviation. The NLO contributions play an important role in understanding the observed pattern of branching ratios of the four $B \rightarrow K\eta^{(\prime)}$ decays.

It is easy to calculate the direct CP-violating asymmetries for the considered decays, which are listed in Table 2. As a comparison, we also list currently available data [2] and the corresponding QCDF predictions [14]. As to the CP-violating asymmetries for the neutral decays $B^0 \rightarrow K^0\eta^{(\prime)}$, one can see the numerical results and discussions as given in Ref.[22].

In short, we calculated the branching ratios and CP-violating asymmetries of $B^+ \rightarrow K^+\eta^{(\prime)}$ and $B^0 \rightarrow K^0\eta^{(\prime)}$ decays in the pQCD approach. The partial NLO contributions considered here include: QCD vertex corrections, the quark-loops and the chromo-magnetic penguins.

From our calculations and phenomenological analysis, we found the following results:

- (a) The NLO contributions in the pQCD approach can provide a 70% enhancement to $Br(B \rightarrow K\eta')$, but a 30% reduction to $Br(B \rightarrow K\eta)$. The large branching ratio of $B \rightarrow K\eta'$ decays, as well as the large disparity $Br(B \rightarrow K\eta') \gg Br(B \rightarrow K\eta)$ can therefore be understood naturally.

Table 2: The pQCD predictions for the direct CP asymmetries in the NDR scheme (in units of 10^{-2}), the QCDF predictions [14] and the world average as given by HFAG [2].

Mode	LO	+VC	+QL	+MP	NLO	Data	QCDF
$\mathcal{A}_{CP}^{dir}(B^\pm \rightarrow K^\pm \eta)$	9.3	31.1	7.8	7.6	-11.7	-27 ± 9	$-18.9^{+29.0}_{-30.0}$
$\mathcal{A}_{CP}^{dir}(B^\pm \rightarrow K^\pm \eta')$	-10.1	-10.6	-5.9	-10.4	-6.2	1.6 ± 1.9	$-9.0^{+10.6}_{-16.2}$

(b) The pQCD predictions for the CP asymmetries of $B \rightarrow K\eta^{(\prime)}$ decays are consistent with currently available data.

(c) One should note that Only the partial NLO contributions in the pQCD approach have been taken into account here. To achieve a complete NLO calculations in the pQCD approach, of course, the still missing pieces should be evaluated as soon as possible.

Acknowledgments

This work is partly supported by the National Natural Science Foundation of China under Grant No.10575052 and 10735080.

References

- [1] B.H. Behrens, CLEO Collaboration, Phys. Rev. Lett. **80**, 3710 (1998).
- [2] E. Barberio *et al.*, (Heavy Flavor Averaging Group), arXiv:0704.3575 [hep-ex] and online update at <http://www.slac.stanford.edu/xorg/hfag>
- [3] P. Chang *et al.*, (Belle Collaboration), Phys. Rev. D **71**, 091106(R) (2005); K.-F. Chen *et al.*, (Belle Collaboration), Phys. Rev. Lett. **98**, 031802 (2007); B. Aubert *et al.*, (BaBar Collaboration), Phys. Rev. D **76**, 031103(R) (2007); Phys. Rev. Lett. **98**, 031801 (2007).
- [4] H.J. Lipkin, Phys. Lett. B **254**, 247 (1991); Y. Grossman and M.P. Worah, Phys. Lett. B **395**, 241 (1997).
- [5] D. Atwood and A. Soni, Phys. Lett. B **405**, 150 (1997); W.S. Hou and B. Tseng, Phys. Rev. Lett. **80**, 434 (1998).
- [6] F. Yuan and K.T. Chao, Phys. Rev. D **56**, R2495 (1997); I. Halperin and A. Zhitnitsky, Phys. Rev. D **56**, 7247 (1997); Phys. Rev. Lett. **80**, 438 (1998).
- [7] A. Ali, J. Chay, C. Greub, and P. Ko, Phys. Lett. B **424**, 161 (1998).
- [8] D.S. Du, C.S. Kim, Y.D. Yang, Phys. Lett. B **426**, 133 (1998).
- [9] M.Z. Yang and Y.D. Yang, Nucl. Phys. B **609**, 469 (2001).
- [10] M.R. Ahmady, E. Kou, A. Sugamoto, Phys. Rev. D **58**, 014015 (1998).
- [11] A.L. Kagan and A.A. Petrov, hep-ph/9707354; S. Khalil and E. Kou, Phys. Rev. Lett. **91**, 241602 (2003).
- [12] G.R. Lu, Z.J. Xiao, H.K. Guo and L.X. Lü, J. Phys. G **25**, L85 (1999); Z.J. Xiao, K.T. Chao and C.S. Li, Phys. Rev. D **65**, 114021(2002); Z.J. Xiao and W.J. Zou, Phys. Rev. D **70**, 094008 (2004).

- [13] M. Beneke and M. Neubert, Nucl. Phys. B **651**, 225 (2003).
- [14] M. Beneke and M. Neubert, Nucl. Phys. B **675**, 333 (2003).
- [15] E. Kou and A. Sanda, Phys. Lett. B **525**, 240 (2002).
- [16] M. Beneke, G. Buchalla, M. Neubert, and C.T. Sachrajda, Phys. Rev. Lett. **83**, 1914 (1999);
- [17] H.N. Li, Prog. Part. & Nucl. Phys. **51**, 85 (2003) and references therein.
- [18] Y.Y. Charng, T. Kurimoto, and H.N. Li, Phys. Rev. D **74**, 074024 (2006); *Erratum* Phys. Rev. D **78**, 059901(E) (2008).
- [19] H.N. Li, S. Mishima, A.I. Sanda, Phys. Rev. D **72**, 114005 (2005).
- [20] G. Buchalla, A.J. Buras, and M.E. Lautenbacher, Rev. Mod. Phys. **68**, 1125 (1996).
- [21] C.D. Lü, K. Ukai and M.Z. Yang, Phys. Rev. D **63**, 074009 (2001).
- [22] Z.J. Xiao, Z.Q. Zhang, X. Liu and L.B. Guo, Phys. Rev. D **78**, 114001 (2008).
- [23] P. Ball, V.M. Braun, Y. Koike, and K. Tanaka, Nucl. Phys. B **529**, 323 (1998); P. Ball, J. High Energy Phys. 9809 (1998) 005; J. High Energy Phys. 9901 (1999) 010; P. Ball and R. Zwicky, Phys. Rev. D **71**, 014015 (2005); J. High Energy Phys. 0604 (2006) 046.
- [24] Particle Data Group, W.-M. Yao *et al.*, J. Phys. G **33**, 1 (2006).